

1 **TITLE:**  
2 Design and Implementation of a Bespoke Robotic Manipulator for Extra-corporeal Ultrasound  
3

4 **AUTHORS AND AFFILIATIONS:**  
5 Shuangyi Wang<sup>1\*</sup>, James Housden<sup>1\*</sup>, Yohan Noh<sup>1</sup>, Anisha Singh<sup>2</sup>, Junghwan Back<sup>3</sup>, Lukas  
6 Lindenroth<sup>3</sup>, Hongbin Liu<sup>3</sup>, Joseph Hajnal<sup>1</sup>, Kaspar Althoefer<sup>4</sup>, Davinder Singh<sup>2</sup>, Kawal Rhode<sup>1</sup>  
7

8 <sup>1</sup>School of Biomedical Engineering & Imaging Sciences, King's College London, UK

9 <sup>2</sup>Xtronics Ltd., Gravesend, UK

10 <sup>3</sup>Department of Informatics, King's College London, UK

11 <sup>4</sup>Faculty of Science & Engineering, Queen Mary University of London, UK

12 \* Both authors contributed equally to this manuscript.  
13

14 **Corresponding Author:**

15 Shuangyi Wang

16 shuangyi.wang@kcl.ac.uk

17 Tel: +44 (0) 7835234417  
18

19 **Email Addresses of Co-authors:**

20 James Housden (richard.housden@kcl.ac.uk)

21 Yohan Noh (yohan.noh@kcl.ac.uk)

22 Anisha Singh (lucky@xtronics.co.uk)

23 Junghwan Back (junghwan.back@kcl.ac.uk)

24 Lukas Lindenroth (lukas.lindenroth@kcl.ac.uk)

25 Hongbin Liu (hongbin.liu@kcl.ac.uk)

26 Joseph Hajnal (jo.hajnal@kcl.ac.uk)

27 Kaspar Althoefer (k.althoefer@qmul.ac.uk)

28 Davinder Singh (xtronics@me.com)

29 Kawal Rhode (kawal.rhode@kcl.ac.uk)  
30

31 **KEYWORDS:**

32 Medical robot, robotic ultrasound, extra-corporeal ultrasound, robot design, mechanism design,  
33 linkages and manipulators, robot safety, 3D-printing, rapid prototyping.  
34

35 **SUMMARY:**

36 This paper introduces the design and implementation of a bespoke robotic manipulator for extra-  
37 corporeal ultrasound examination. The system has five degrees-of-freedom with lightweight  
38 joints made by 3D printing and a mechanical clutch for safety management.  
39

40 **ABSTRACT:**

41 With the potential for high precision, dexterity, and repeatability, a self-tracked robotic system  

---

42 can be employed to assist the acquisition of real-time ultrasound. However, limited numbers of  
43 robots designed for extra-corporeal ultrasound have been successfully translated into clinical use.  
44 In our study, we aim to build a bespoke robotic manipulator for extra-corporeal ultrasound  
45 examination, which is lightweight and has a small footprint. The robot is formed of five specially-  
46 shaped links and custom-made joint mechanisms for probe manipulation to cover the necessary  
47 range of motion with redundant degrees-of-freedom to ensure patient safety. The mechanical  
48 safety is emphasized with a clutch mechanism to limit the force applied to patients. As a result  
49 of the design, the total weight of the manipulator is less than 2 kg and the length of the  
50 manipulator is about 25 cm. The design has been implemented, and simulation, phantom and  
51 volunteer studies performed, to validate the range of motion, ability to make fine adjustments,  
52 mechanical reliability, and safe operation of the clutch. This paper details the design and  
53 implementation of the bespoke robotic ultrasound manipulator with the design and assembly  
54 methods illustrated. Testing results to demonstrate the design features and clinical experience  
55 of using the system are presented. It is concluded that the current proposed robotic manipulator  
56 meets the requirements as a bespoke system for extra-corporeal ultrasound examination and  
57 has great potential to be translated into clinical use.

58

## 59 **INTRODUCTION:**

60 An extra-corporeal robotic ultrasound (US) system refers to the configuration in which a robotic  
61 system is utilized to hold and manipulate an US probe for external examinations, including use in  
62 cardiac, vascular, obstetric, and general abdominal imaging<sup>1</sup>. The use of such a robotic system is  
63 motivated by the challenges of manually holding and manipulating a US probe: e.g. the challenge  
64 of finding standard US views required by clinical imaging protocols and the risk of repetitive strain  
65 injury<sup>2-4</sup>, and also by the needs of US screening programs: e.g. the requirement for experienced  
66 sonographers to be on-site<sup>5,6</sup>. With emphases on different functionalities and target anatomies,  
67 several robotic US systems, as reviewed in the works<sup>1,7,8</sup>, have been introduced since the 1990s  
68 to improve different aspects of US examination: e.g. long-distance tele-operation<sup>9-12</sup>, as well as  
69 robot-operator interaction and automatic control<sup>13,14</sup>. In addition to the robotic US systems used  
70 for diagnostic purpose, robotic high intensity focused ultrasound (HIFU) systems for treatment  
71 purposes have been widely investigated as summarized in<sup>1</sup>, with some of the recent works such  
72 as<sup>15,16</sup> reported for the latest progress.

73

74 Although several robotic US systems have been developed with relatively reliable technologies  
75 for control and clinical operation, only a few of them have been successfully translated into  
76 clinical use, such as the commercially-available system from<sup>17</sup>. One possible reason is the low  
77 level of acceptance for large-size industrial-looking robots working in a clinical environment, from  
78 the point of view of both patients and sonographers. Additionally, for safety management, the  
79 majority of the existing US robots rely on force sensors to monitor and control the applied  
80 pressure to the US probe, while more fundamental mechanical safety mechanisms to limit the  
81 force passively are usually not available. This may also cause concerns when translating into  
82 clinical use as the safety of robot operation would be purely dependent on electrical systems and  
83 software logic.

84

85 With the recent advancements of 3D printing techniques, specially-shaped plastic links with  
86 custom-made joint mechanisms could provide a new opportunity for developing bespoke  
87 medical robots. Carefully designed lightweight components with a compact appearance could  
88 improve the clinical acceptance. Specifically for US examination, a bespoke medical robot aimed  
89 to be translated into clinical use should be compact, with enough degrees-of-freedom (DOFs) and  
90 range of motion to cover the region of interest of a scan; for example, the abdominal surface  
91 including both the top and sides of the belly. Additionally, the robot should also incorporate the  
92 ability to do fine adjustments of the US probe in a local area, when trying to optimize an US view.  
93 This usually includes tilting movements of the probe within a certain range as suggested in<sup>18,19</sup>.  
94 To further address the safety concerns, it is expected that the system should have passive  
95 mechanical safety features which are independent of electrical systems and software logic.

96  
97 In this paper, we present the detailed design and assembly method of a 5-DOF dexterous robotic  
98 manipulator, which is used as the key component of an extra-corporeal robotic US system. The  
99 manipulator consists of several lightweight 3D-printable links, custom-made joint mechanisms,  
100 and a built-in safety clutch. The specific arrangement of DOFs provides full flexibility for probe  
101 adjustments, allowing easy and safe operation in a small area without colliding with the patient.  
102 The proposed multi-DOF manipulator aims to work as the main component that is in contact with  
103 patients and it can be simply attached to any conventional 3-DOF global positioning mechanism  
104 to form a complete US robot with fully active DOFs to perform an US scan.

## 105 106 **PROTOCOL:**

107  
108 1. Print all the links ( $L_0$ ,  $L_1$ ,  $L_2$ ,  $L_3$ , and  $L_4$ ) and the end-effector as shown in **Figure 1** with ABS  
109 (acrylonitrile butadiene styrene) plastic, PLA (polylactic Acid) plastic, or Nylon using a 3D printing  
110 service. Use the STL files provided in the supplementary materials when printing.

111  
112 Note: changes in shape and scale of each part can be made based on the provided files. The inner  
113 profile of the end-effector can be changed to fit different US probes.

114  
115 2. Print all the required additional components as shown in **Figure 2** in Nylon using a 3D printing  
116 service. Refer to the material list for the required number of each component. Use the STL files  
117 provided in the supplementary materials when printing.

118  
119 3. Polish all the printed plastic parts with polishing tools if necessary. Remove supporting  
120 materials left from 3D printing if necessary.

121  
122 Note: some structures in the provided end-effector design are for a force sensor, which is not a  
123 part of the current reported protocol and will not be used for the assembly. The force sensor  
124 design concept has been reported in previous work<sup>20</sup>, thus it is not covered in this paper.

125  
126 3. Assembly of Joint 1 ( $J_1$ ) based on **Figure 3:**

127  
128 3.1. Place the four small geared stepper motors (with 20-teeth spur gears attached) into the

129 mounting cavities of  $L_0$  and mount them with screws.

130

131 3.2. Place the two 37 mm O.D bearings into the bearing housings of  $L_0$  and secure the 120-teeth  
132 spur gear (Type A) onto the hexagon key of  $L_1$ .

133

134 3.3. Insert the shaft on  $L_1$  into the shaft hole on  $L_0$  with the four small driving spur gears and the  
135 large driven spur gear engaged and assemble the shaft collar to secure and retain the shaft.

136

137 4. Assembly of Joint 2 ( $J_2$ ) based on **Figure 4:**

138

139 4.1 Place the four small geared stepper motors (with 20-teeth spur gears attached) into the  
140 mounting cavities of  $L_1$  and mount them with screws.

141

142 4.2. Attach the two 120-teeth spur gears (Type B) to the two 37 mm O.D bearings and position  
143 them into the gear cavities of  $L_1$ , with the 120-teeth spur gear (Type B) engaged with the 20-teeth  
144 spur gears mounted on the motors.

145

146 4.3. Insert the four ball-spring pairs into the clutch holes in  $L_2$  with the two round clutch covers  
147 pushing the spring into the clutch mechanism for pre-loading.

148

149 4.4. Insert the shaft (e.g. an M6 bolt with a nut) into the bores of  $L_1$  and  $L_2$  with the two joints  
150 properly aligned and place the two 12 mm O.D bearings into the bearing housings of  $L_2$ .

151

152 5. Assembly of Joint 3 ( $J_3$ ) based on **Figure 5:**

153

154 5.1. Place the two small geared stepper motors (with 20-teeth spur gears attached) into the  
155 mounting cavities of  $L_2$  and mount them with screws.

156

157 5.2. Place the 37 mm O.D bearing into the bearing housing of the 120-teeth spur gear (Type C)  
158 and place the 32 mm O.D bearing into the bearing housing of  $L_3$ .

159

160 5.3. Secure the large spur gear into the hexagon keyhole of  $L_3$  (additional screws can be used if  
161 necessary) and insert the shaft on  $L_2$  into the bores on the large spur gear and  $L_3$ , with the small  
162 and the large spur gears engaged. Ensure the driven large spur gear rotates freely on the 37 mm  
163 O.D bearing and  $L_3$  rotates freely on the 32 mm O.D bearing.

164

165 6. Assembly of Joint 4 ( $J_4$ ) based on **Figure 6:**

166

167 6.1. Place the two small geared stepper motors into the mounting cavities of  $L_3$  and mount them  
168 with screws. Place the 8 mm O.D bearings into the bearing housings of  $L_4$ .

169

170 6.2. Mount the 20-teeth long spur gear onto the two small stepper motors and insert the shaft  
171 into the shaft hole of  $L_3$  and  $L_4$  after the two links are aligned (e.g. using an M5 bolt with a nut).  
172 Ensure the built-in driven gear structure on  $L_4$  mates with the 20-teeth long spur gear.

173

174 7. Assembly of Joint 5 ( $J_5$ ) based on **Figure 7**:

175

176 7.1. Place the two small geared stepper motors (with 18-teeth bevel gears attached) into the  
177 mounting cavities of  $L_4$  and mount them with screws.

178

179 7.2. Position the driving 144-teeth bevel gear onto the extrusion of  $L_4$  with its bottom gear part  
180 engaged with the two driving small bevel gears.

181

182 7.3. Insert the end-effector into the keyway of the large bevel gear and vertically position the  
183 end-effector with the end-effector collar screwed onto it. Ensure the end-effector collar, rotating  
184 on the top round surface of  $L_4$ , holds and positions the end-effector vertically.

185

### 186 **REPRESENTATIVE RESULTS:**

187 Following the protocol, the resulting system is a robotic manipulator with five specially-shaped  
188 links ( $L_0$  to  $L_4$ ) and five revolute joints ( $J_1$  to  $J_5$ ) for moving, holding and locally tilting an US probe  
189 (**Figure 8**). The top rotation joint ( $J_1$ ), with gear mechanisms actuated by four motors, can rotate  
190 the following structures 360 degrees to allow the US probe to point towards different sides of  
191 the scanning area, such as the top, bottom, and sides of the abdomen. The main tilting joint ( $J_2$ ),  
192 with gear mechanisms actuated by four motors, is used to tilt down the probe to align with the  
193 surface of the scanning area. As this joint is also crucial to the force management, a mechanical  
194 clutch with balls, springs, and detent holes was incorporated. The last three orthogonal revolute  
195 joints ( $J_3$ ,  $J_4$ , and  $J_5$ ), with gear mechanisms actuated by two motors each, are used to control the  
196 tilting and axial rotation of the probe, allowing fine adjustments of the probe in a local area. The  
197 last revolute joint  $J_5$  also allows the mounting of an US probe in a specially-shaped end-effector.  
198 The total weight and length of the proposed robotic manipulator, which is the only structure  
199 usually on top of the patient's body, are less than 2 kg and 25 cm. The resulting design is such  
200 that a large range of probe positions can be reached with only small movements of the remaining  
201 global positioning mechanism when using the proposed robotic US manipulator. Considering just  
202 the proposed manipulator on its own, the probe can be rotated axially to any angle, tilted to  
203 follow a surface angled between 0 and 110 degrees to the horizontal in any direction, and  
204 positioned within a circle of diameter 360 mm. Additionally, the revolute joints  $J_3$  and  $J_4$  provide  
205 a tilting angle in the range -180 to 180 degrees and -30 to 45 degrees, respectively in two  
206 directions, which is used for local fine adjustments of the US probe. The ranges of movements  
207 and tilting angles meet the required ranges for obtaining an ideal acoustic window for US  
208 examinations as suggested in<sup>18,19</sup>. The technical details of the proposed robotic manipulator are  
209 summarized in Table 1 (Denavit–Hartenberg parameters and joint specifications) based on the  
210 coordinate definitions shown in **Figure 8**. The estimated cost of the system is 500 GBP based on  
211 the current manufacturing method, components and materials.

212

213 As an example used in this research, we employed a global positioning system which has a  
214 revolute joint ( $R_1$ ) with a chain mechanism for rotating the complete arm and a two-bar arm-  
215 based set of parallel link mechanisms ( $R_2$  and  $R_3$ ) with worm-gear drives (**Figure 9**). This 3-DOFs  
216 mechanism will work with the proposed 5-DOF manipulator to form a complete robotic US

217 system. Based on the proposed robotic manipulator and the example global positioning option  
218 used for this research, **Figure 10** shows a simulation example of the robot in positions around an  
219 abdominal phantom, demonstrating that it is able to reach around both sides of the abdomen  
220 and a range of positions on top. The design of the redundant joints in the system, particularly the  
221 configurations of  $J_1$  and  $J_2$ , allows tilting the probe to large angles with most of the mechanical  
222 structures still staying away from the patient's body, as can be observed from **Figure 10**.  
223 Consequently, with the last three joints ( $J_3$ ,  $J_4$ , and  $J_5$ ) specified to rotate within limited ranges for  
224 fine tilting adjustments, collision is avoided between the moving parts of the robot and the  
225 patient's body.

226  
227 With the electronics and the conventional stepper motor control system developed, experiments  
228 have been performed to test the output force and validate the expected range of motion. The  
229 current control unit is a box with microcontrollers, stepper motor drivers, power supply and  
230 regulators, and other supporting electronic components included. The overall size of the control  
231 box is 40 cm long, 23 cm wide and 12 cm deep. Based on the repeated testing of the system, the  
232 maximum force that the robotic manipulator can currently exert is set to 27 N before the  
233 mechanical safety clutch is triggered, specifying the output force range of the proposed system  
234 to be 0 N to 27 N. With the configuration of the mechanical clutch, it was verified by repeated  
235 testing that in the default position when the clutch is engaged, the balls are partially in the detent  
236 holes of  $L_1$ . Therefore the movements of the driven large spur gears actuate  $L_2$ . However, when  
237 excessive force is exerted at the end-effector, the clutch is disengaged with the balls moving out  
238 of the detent holes of  $L_1$ .

239  
240 The range of motion of each joint reported in Table 1 was also repeatedly tested and validated.  
241 The reliable working of the robotic manipulator over a long period of time has been extensively  
242 tested on a fetal phantom and continuously verified with abdominal scans of internal healthy  
243 volunteers (**Figure 11**). The study was approved by the local ethics committee. So far, 20  
244 volunteer scans for general abdominal ultrasound examinations using the robotic manipulator  
245 have been successfully performed with basic software control of the robot, mainly to evaluate  
246 the reliability and feasibility of the mechanical design. It was concluded from the phantom and  
247 volunteers studies that the current design of the robotic manipulator can reach the required  
248 movement range at the required force, and provides enough fine adjustment, to obtain images  
249 similar to the hand-held operation of the US probe for abdominal imaging. For all these scans, no  
250 safety concerns or uncomfortable feelings were reported by the volunteers. The selection of  
251 motors, mechanical ratios of mechanisms, and power levels, have been verified such that they  
252 ensure the reliable movement of the probe on the patient's body, while at the same time  
253 resulting in slippage if exceeded forces are generated. Further details of this on-going volunteer  
254 study and clinical evidence for the use of the robot will be presented separately.

## 255 **FIGURE AND TABLE LEGENDS:**

256  
257  
258 **Figure 1: CAD drawing of all the links ( $L_0$ ,  $L_1$ ,  $L_2$ ,  $L_3$ , and  $L_4$ ) and the end-effector.** The shape of  
259 each link is shown for reference when 3D printing using the provided STL files. The end-effector  
260 is illustrated with an US probe included in the assembly.

261

262 **Figure 2: CAD drawing of the required additional components.** The shape of each component is  
263 shown for reference when 3D printing using the provided STL files. The components include spur  
264 and bevel gears in different sizes, shaft collar, clutch cover, and end-effector collar.

265

266 **Figure 3: Assembly instruction for  $J_1$ .** The required links, motors, gears, and bearings are shown  
267 with some structures changed to transparent to illustrate the assembly.

268

269 **Figure 4: Assembly instruction for  $J_2$ .** The required links, motors, gears, ball-spring pairs, and  
270 bearings are shown with some structures changed to transparent to illustrate the assembly.

271

272 **Figure 5: Assembly instruction for  $J_3$ .** The required links, motors, gears, and bearings are shown  
273 with two perspective views to illustrate the assembly.

274

275 **Figure 6: Assembly instruction for  $J_4$ .** The required links, motors, gears, and bearings are shown  
276 with the assembled  $J_4$  mechanism indicated.

277

278 **Figure 7: Assembly instruction for  $J_5$ .** The required link and end-effector, motors, and gears are  
279 shown with some structures changed to transparent to illustrate the assembly.

280

281 **Figure 8: Summary of the proposed 5-DOF robotic manipulator with the end-effector holding**  
282 **an US probe.** The coordinate definition of each joint and the overall size of the assembled  
283 manipulator are indicated.

284

285 **Figure 9: CAD drawing of the example global positioning device.** This arm-based device is used  
286 to work with the proposed robotic manipulator for testing. The notations and the main  
287 dimensions are shown in the drawing.

288

289 **Figure 10: Kinematic simulation of four different scanning postures around the phantom.** This  
290 demonstrates an adequate range of motion for a typical abdominal US scan.

291

292 **Figure 11: Implemented US robot using the described protocol.** (a) The robotic manipulator with  
293 the example global positioning mechanism; (b) clinical use of the proposed robotic manipulator  
294 on a patient's abdominal area.

295

296 **Table 1: Technical details of the proposed robotic manipulator, including the Denavit–**  
297 **Hartenberg parameters and the joint specifications.**

298

## 299 **DISCUSSION:**

300 Unlike many other industrial robots that have been translated into medical applications, the  
301 proposed robotic manipulator described in the protocol was specifically designed for US  
302 examinations according to the clinical requirements for the range of motion, application of force,  
303 and safety management. The lightweight robotic manipulator itself has a wide range of  
304 movements sufficient for most extra-corporeal US scanning without the need for large

305 movements of the global positioning mechanism. As the closest mechanical structure to the  
306 patient, the proposed links are also specially-shaped to be away from the patient. With most  
307 DOFs embedded into a compact manipulator, robotic US scanning using this device can be done  
308 in an intuitive way similar to human operation without the necessity of occupying a large space.  
309 Because of all these features, we expect the system produced following the protocol could gain  
310 acceptance from the clinicians and patients, which is being validated with the on-going volunteer  
311 study. With the proposed robotic manipulator, different conventional architectures for global  
312 positioning can be used based on the particular requirement, such as a gantry or ceiling mounting  
313 designs. An example global positioning device was used in this paper to enable the tests of the  
314 proposed robotic manipulator.

315  
316 The current protocol suggests that all the links can be printed using ABS or PLA plastics, or Nylon  
317 based on the availability of the local 3D printing service, while using the Nylon prints is preferred  
318 in general due to its material strength. Importantly as stated in the protocol, the additional  
319 components, especially the gears, should be printed with Nylon or other strong materials to  
320 ensure the reliability of the system. As new 3D printing materials are introduced, the use of  
321 materials could be altered. The current protocol employs an end-effector specifically designed  
322 for a particular US probe with the probe's 3D shape scanned by a CT imaging system to assist the  
323 design of the inner profile of the end-effector. When the manipulator is used with other US  
324 probes with different shapes, it is important to ensure that the inner profile of the end-effector  
325 is re-designed to tightly mate with the outer profile of the US probe, in order to guarantee the  
326 safe holding of the probe. The 3D shape and profile of the probe could also be obtained from  
327 other types of 3D scanning. Additionally, it should be noted that some of the design details  
328 described in the protocol, such as exact shapes and dimensions, shaft sizes, mounting keyways,  
329 screws, and use of bearings, could be altered. For the same reason, some of the details are not  
330 provided when it is obvious based on common knowledge of mechanical design.

331  
332 The current design has a passive mechanical clutch which can be adjusted and used to limit the  
333 maximum force applied to the patient. This is a safety feature that does not rely on any electrical  
334 systems or software logic, which guarantees the fundamental safety for using the robot for US  
335 examinations. The triggering point was set based on the range from our previous  
336 measurements<sup>21</sup> of the vertical force applied by human operators to the patients during normal  
337 US scans as well as similar results reported from the existing literature<sup>18</sup>, both of which suggest  
338 that the maximum vertical force usually does not exceed 20 N. This was treated as the  
339 prerequisite that the trigger force of the clutch should be more than 20 N with some given  
340 allowances. The amount of triggering force can be adjusted by changing the number of ball-spring  
341 pairs, the spring constant, the size of the detent holes, and the pre-loading of the springs<sup>22</sup>. A  
342 potential modification of the designed protocol for this is to change the numbers of cavities for  
343 holding the ball-spring pairs in  $L_2$ . In practice when using the proposed system, the correct  
344 working of the clutch can be easily verified by manually rotating the clutch joint and having the  
345 clutch disengage and re-engage before any robotic US examination is performed. In the current  
346 protocol, the safety clutch is only applied to  $J_2$  as this joint is designed to align the probe with the  
347 surface of the abdomen and can be directly used to limit the vertical force exerted on the patient  
348 by the US probe. With a similar concept, a safety clutch can also be implemented for the  $J_1$  spur



349 gear, which will ensure the safety of the  $J_1$  rotational movement of the following structures. This  
350 is not seen as an essential safety feature in the current protocol, but could be a potential  
351 modification for a finalized version. The last three joints  $J_3$ ,  $J_4$ , and  $J_5$  are used for fine adjustments  
352 of the probe's orientation. Kinematically, they are not used to generate any excessive force and  
353 are not likely to collide with any obstacle. To minimize the size and weight of the proposed  
354 manipulator, a safety mechanical clutch is not suggested for these three joints in any modification  
355 of the protocol.

356  
357 Following the proposed protocol to build the proposed manipulator for US examinations, the  
358 same reliability of the mechanical system, the same ranges of motion, similar weights of the  
359 whole manipulator, and a similar level of triggering force of the clutch are expected as are  
360 reported in this paper. However, the repeatability and accuracy of the movements, as well as the  
361 repeatability of the exact triggering force level of the mechanical clutch, would strongly depend  
362 on the 3D-printing and assembly accuracy compared to the CAD design. This cannot be  
363 guaranteed for the current prototype as a lab-based low-end 3D printing service was used for  
364 manufacturing and the assembly was done manually for the purpose of preliminary prototyping.  
365 It is expected that an industrial level of manufacturing and assembly following the design  
366 protocol would result in good repeatability and high accuracy, although this is not our currently  
367 our aim before the system is made into a final product for clinical trial. Testing of the performance  
368 would also require a separate protocol, which includes kinematic modelling, a robotic control  
369 method, motion tracking and calibration methods, and is thus not included in the current paper.  
370 Similarly, the control precision and response of the proposed manipulator are determined by the  
371 motor control method, robot control algorithm, and communication between the electronics of  
372 the manipulator and the control interface. As these are beyond the aim of the current protocol  
373 of introducing the new mechanical design and can be implemented using many existing  
374 architectures, details are not provided in this paper.

375

#### 376 **ACKNOWLEDGMENTS:**

377 This work was supported by the Wellcome Trust IEH Award [102431] and by the Wellcome/EPSRC  
378 Centre for Medical Engineering [WT203148/Z/16/Z]. The authors acknowledge financial support  
379 from the Department of Health via the National Institute for Health Research (NIHR)  
380 comprehensive Biomedical Research Centre award to Guy's & St Thomas' NHS Foundation Trust  
381 in partnership with King's College London and King's College Hospital NHS Foundation Trust.

382

#### 383 **DISCLOSURES:**

384 The authors have nothing to disclose.

385

#### 386 **REFERENCES:**

- 387 1. Priester, A. M., Natarajan, S., Culjat, M. O. Robotic ultrasound systems in medicine. *IEEE*  
388 *transactions on ultrasonics, ferroelectrics, and frequency control*. **60** (3), 507-523 (2013).
- 389 2. Magnavita, N., Bevilacqua, L., Mirk, P., Fileni, A., Castellino, N. Work-related musculoskeletal  
390 complaints in sonologists. *Journal of occupational and environmental medicine*. **41** (11), 981-988  
391 (1999).
- 392 3. Jakes, C. Sonographers and Occupational Overuse Syndrome: Cause, Effect, and Solutions.

393 *Journal of Diagnostic Medical Sonography*. **17** (6), 312-320 (2001).

394 4. Society of Diagnostic Medical Sonography. Industry Standards for the Prevention of Work-

395 Related Musculoskeletal Disorders in Sonography: Consensus Conference on Work-Related

396 Musculoskeletal Disorders in Sonography. *Journal of Diagnostic Medical Sonography*. **27** (1), 14-

397 18 (2011).

398 5. LaGrone, L. N., Sadasivam, V., Kushner, A. L., Groen, R. S. A review of training opportunities for

399 ultrasonography in low and middle income countries. *Tropical medicine & international health:*

400 *TM & IH*. **17** (7), 808-819 (2012).

401 6. Shah, S. et al. Perceived barriers in the use of ultrasound in developing countries. *Critical*

402 *ultrasound journal*. **7** (1), 28 (2015).

403 7. Swerdlow, D. R., Cleary, K., Wilson, E., Azizi-Koutenaie, B., Monfaredi, R. Robotic Arm-Assisted

404 Sonography: Review of Technical Developments and Potential Clinical Applications. *American*

405 *Journal of Roentgenology*. **208** (4), 733-738 (2017).

406 8. Nouaille, L., Laribi, M., Nelson, C., Zeghloul, S., Poisson, G. Review of Kinematics for Minimally

407 Invasive Surgery and Tele-Echography Robots. *Journal of Medical Devices*. **11** (4), 040802 (2017).

408 9. Georgescu, M., Sacccomandi, A., Baudron, B., Arbeille, P. L. Remote sonography in routine

409 clinical practice between two isolated medical centers and the university hospital using a robotic

410 arm: a 1-year study. *Telemedicine and e-Health*. **22** (4), 276-281 (2016).

411 10. Arbeille, P. et al. Use of a robotic arm to perform remote abdominal telesonography.

412 *American journal of Roentgenology*. **188** (4), W317-W322 (2007).

413 11. Arbeille, P. et al. Fetal tele-echography using a robotic arm and a satellite link. *Ultrasound in*

414 *obstetrics & gynecology*. **26** (3), 221-226 (2005).

415 12. Vieyres, P. et al. A tele-operated robotic system for mobile tele-echography: The OTELO

416 project. *M-Health*. Springer, Boston, MA. 461-473 (2006).

417 13. Abolmaesumi, P., Salcudean, S. E., Zhu, W.H., Sirouspour, M. R., DiMaio, S. P. Image-guided

418 control of a robot for medical ultrasound. *IEEE Transactions on Robotics and Automation*. **18** (1),

419 11-23 (2002).

420 14. Abolmaesumi, P., Salcudean, S., Zhu, W. Visual servoing for robot-assisted diagnostic

421 ultrasound. *Engineering in Medicine and Biology Society, Proceedings of the 22nd Annual*

422 *International Conference of the IEEE*. IEEE. 2532-2535 (2000).

423 15. Menikou, G., Yiallouras, C., Yiannakou, M., Damianou, C. MRI-guided focused ultrasound

424 robotic system for the treatment of bone cancer. *The International Journal of Medical Robotics*

425 *and Computer Assisted Surgery*. **13** (1), e1753 (2017).

426 16. Yiallouras, C. et al. Three-axis MR-conditional robot for high-intensity focused ultrasound for

427 treating prostate diseases transrectally. *Journal of therapeutic ultrasound*. **3** (1), 2 (2015).

428 17. Telemedicine: MELODY, a remote, robotic ultrasound solution.

429 <<http://www.adechotech.com/products/>>. (2018).

430 18. Essomba, T. et al. A specific performances comparative study of two spherical robots for tele-

431 echography application. *Proceedings of the Institution of Mechanical Engineers, Part C: Journal*

432 *of Mechanical Engineering Science*. **228** (18), 3419-3429 (2014).

433 19. Bassit, L. A. Structure me´canique a` modules sphe´riques optimise´es pour un robot me´dical

434 de te´le´-e´chographie mobile. *PhD thesis, Universit´e d'Orl´eans*. (2005).

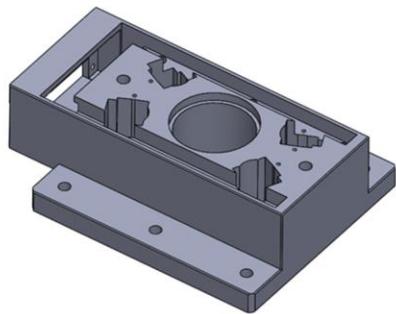
435 20. Noh, Y. et al. Multi-Axis force/torque sensor based on Simply-Supported beam and

436 optoelectronics. *Sensors*. **16** (11), 1936 (2016).

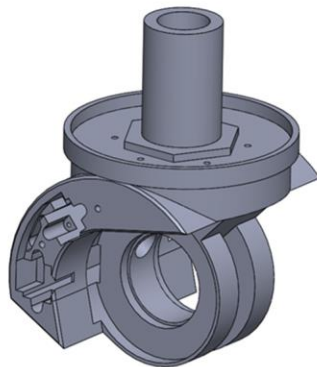
437 21. Noh, Y. et al. An ergonomic handheld ultrasound probe providing contact forces and pose  
438 information. *Engineering in Medicine and Biology Society, Proceedings of the 37th Annual*  
439 *International Conference of the IEEE*. IEEE. 5773-5776 (2015).

440 22. Translational detent component with asymmetric notch geometry.  
441 <[https://www.maplesoft.com/support/help/MapleSim/view.aspx?path=DrivelineComponentLib](https://www.maplesoft.com/support/help/MapleSim/view.aspx?path=DrivelineComponentLibrary/translationalDetent)  
442 [rary/translationalDetent](https://www.maplesoft.com/support/help/MapleSim/view.aspx?path=DrivelineComponentLibrary/translationalDetent)>. (2018).

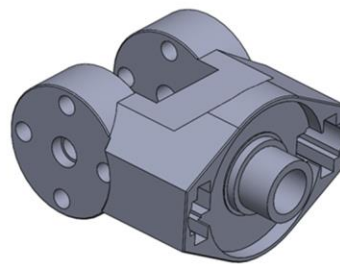
443  
444  
445  
446  
447  
448  
449  
450  
451  
452  
453  
454  
455  
456  
457  
458  
459  
460  
461  
462  
463  
464  
465  
466  
467  
468  
469  
470  
471  
472  
473  
474  
475  
476  
477  
478  
479  
480



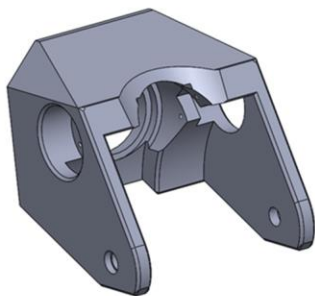
Link 0 ( $L_0$ )



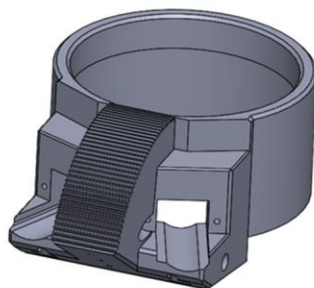
Link 1 ( $L_1$ )



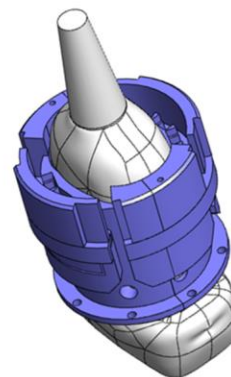
Link 2 ( $L_2$ )



Link 3 ( $L_3$ )



Link 4 ( $L_4$ )



End-effector

481  
482  
483



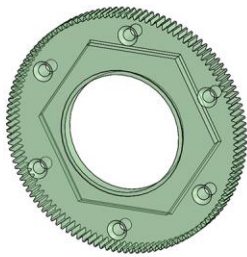
20-teeth spur gear



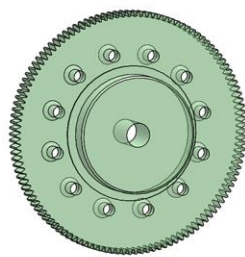
18-teeth bevel gear



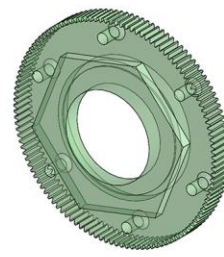
20-teeth long spur gear



120-teeth spur gear (type A)



120-teeth spur gear (type B)



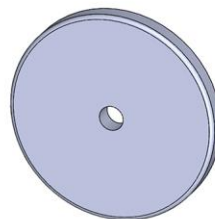
120-teeth spur gear (type C)



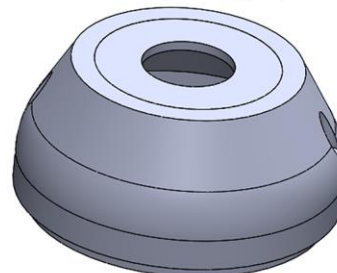
144-teeth bevel gear



Shaft collar (for  $J_1$ )

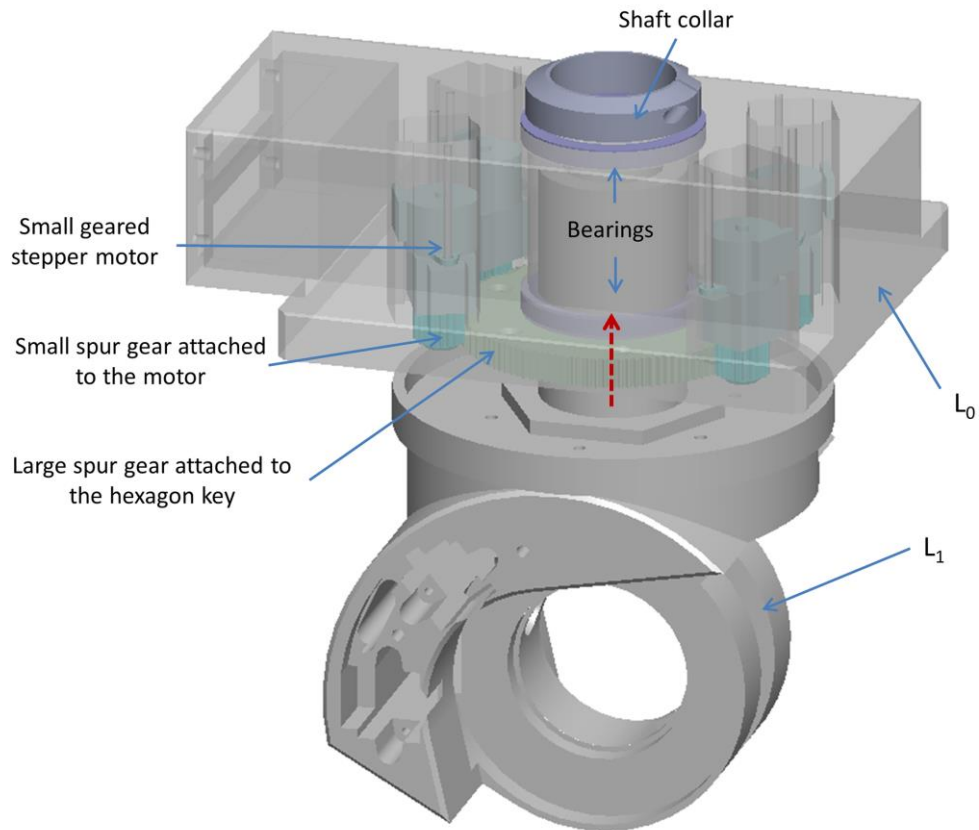


Clutch cover (for  $J_2$ )

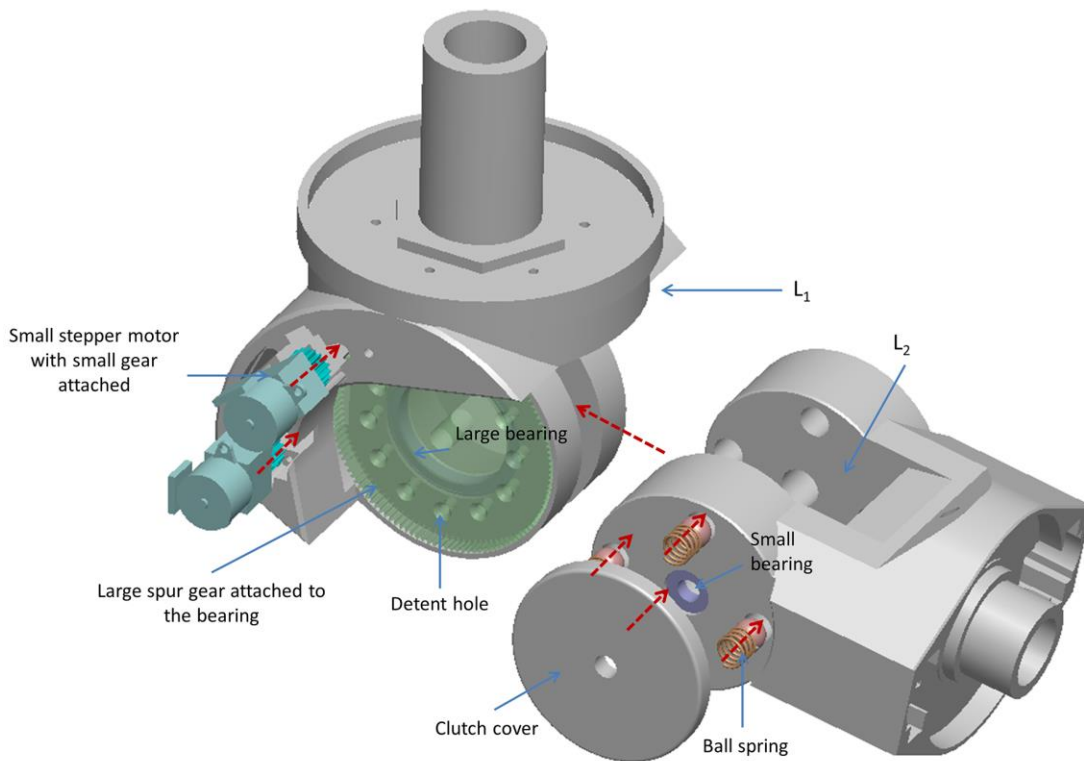


End-effector collar (for  $J_3$ )

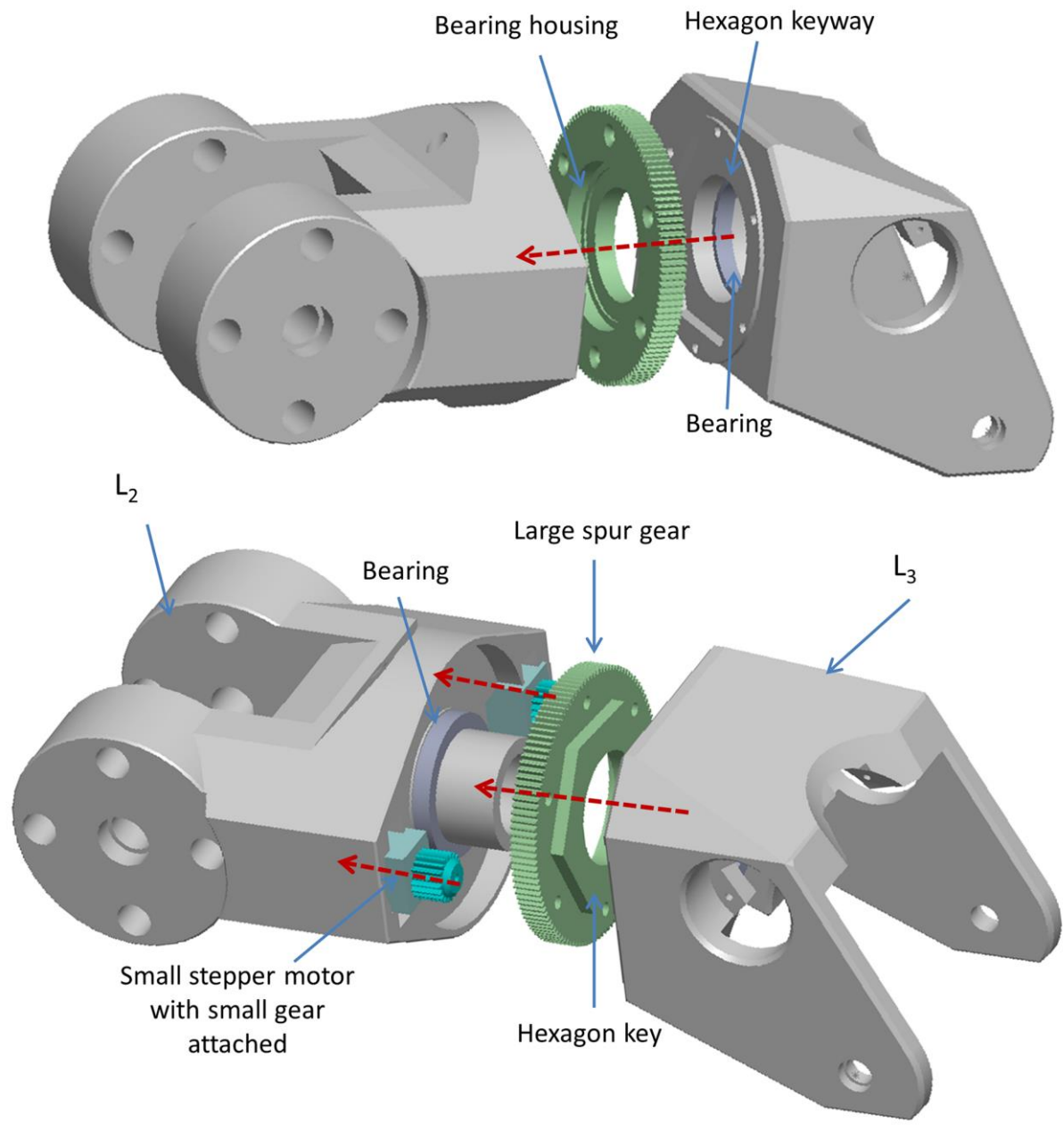
484

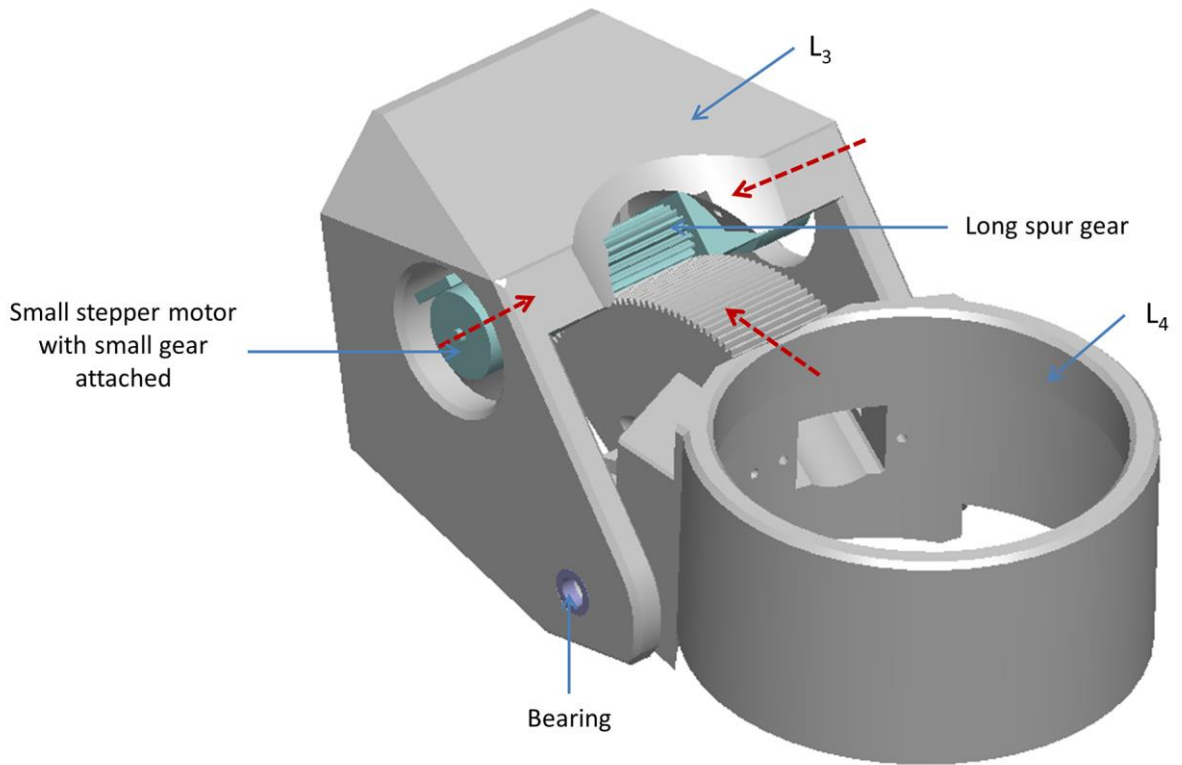


485  
 486  
 487

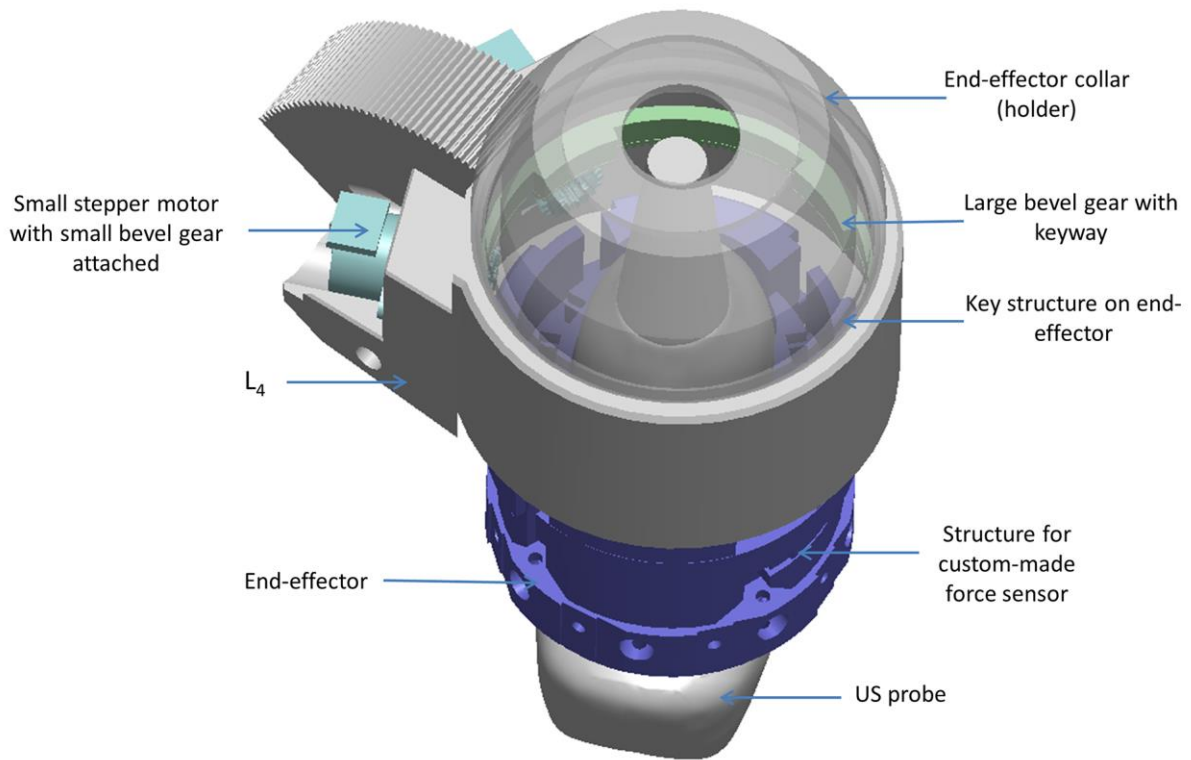


488

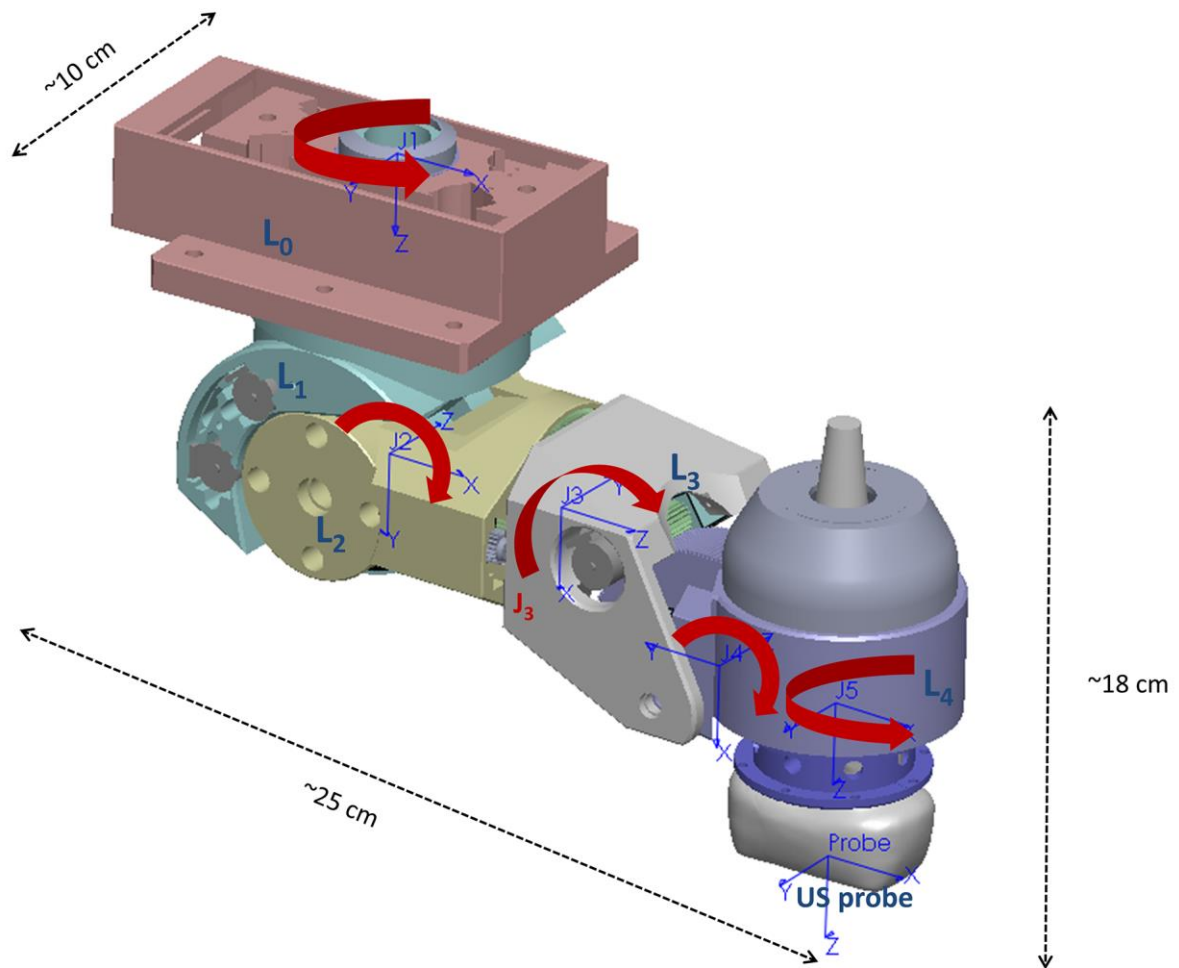




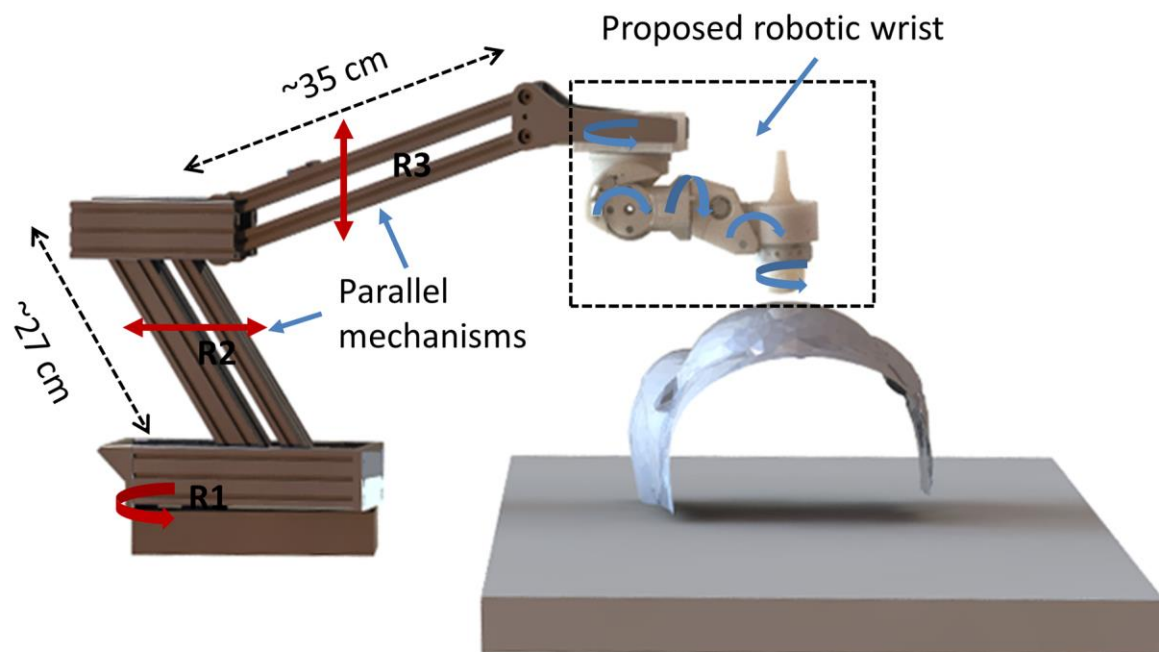
490  
491



492

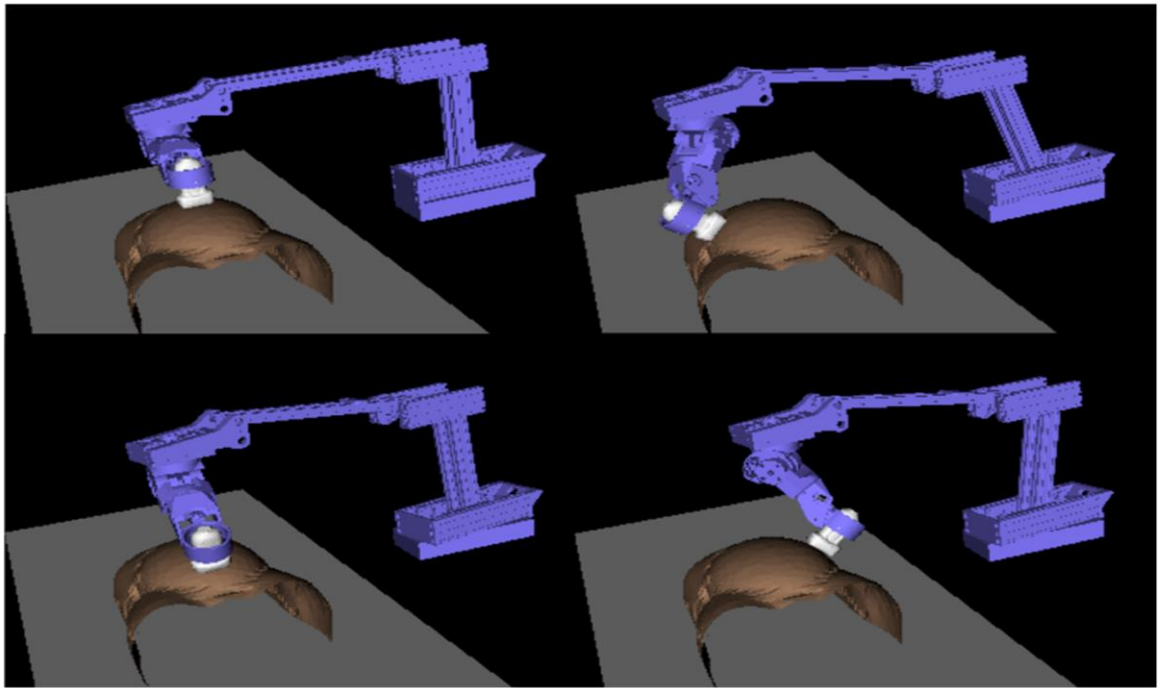


493

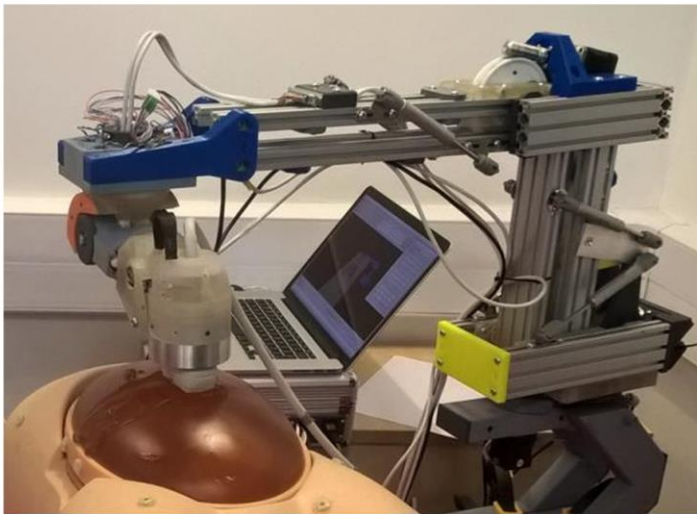


494





495  
496



(a)



(b)

497